Malaysian Journal of Analytical Sciences (MJAS)
Published by Malaysian Analytical Sciences Society

MOLECULAR RECOGNITION OF DIBUTYL PHTHALATE IMPRINTED POLYMER USING METHACRYLIC ACID (MAA) AS FUNCTIONAL MONOMER *via* PRECIPITATION POLYMERIZATION

(Pengecaman Molekul Polimer Tercetak Dibutil Ftalat Menggunakan Asid Metakrilik (MAA) Sebagai Monomer Berfungsi Melalui Pempolimeran Pemendakan)

Nur Adlina Mohd Zaidi[1], Faizatul Shimal Mehamod[2*], Abd Mutalib Md Jani[3], Nur Asyiqin Zulkefli[1], Ana Asyura Mohd Jamal[1], Nur Habibah Safiyah Jusoh[1]

[1]Faculty of Science and Marine Environment Universiti Malaysia Terengganu, 21030 Kuala Nerus, Terengganu, Malaysia
[2]Advanced Nano Materials (ANoMA) Research Group, Faculty of Science and Marine Environment Universiti Malaysia Terengganu, 21030 Kuala Nerus, Terengganu, Malaysia
[3]Faculty of Applied Sciences, Universiti Teknologi MARA, Perak Branch, Tapah Campus, 35400 Perak, Malaysia

**Corresponding author: fshimal@umt.edu.my*

Received: 8 November 2023; Accepted: 4 August 2024; Published: 29 December 2024

Abstract

The extensive utilization of phthalates raises concerns regarding their impact on human and animal well-being. Therefore, this study aimed to explore the potential formation of a molecularly imprinted polymer by examining its physical characteristics and adsorption capabilities through a binding analysis. This study synthesized the dibutyl phthalate-imprinted polymer (DBP-IP) by precipitation polymerization using dibutyl phthalate (DBP), methacrylic acid, and divinylbenzene-80 as the template, functional monomer and crosslinker, respectively. The polymers were characterized using Fourier Transform Infrared spectroscopy, Scanning Electron Microscopy, and surface area and porosity analysis. The performance of the synthesized polymer was evaluated through a batch rebinding experiment. Therefore, the kinetic spectrophotometric method was used to describe the determination of the DBP molecule based on its adsorption effect onto the polymer. The effects of pH, concentration, and time taken were investigated to reveal the possible mechanism through the adsorption isotherm and kinetic study. The findings demonstrated that the DBP-IP has a good adsorption efficiency in acidic solutions with lower concentrations. The maximum percentage removal for DBP-IP and NIP reached 90% and 53%, respectively. Studies on adsorption showed that the DBP-IP followed the Langmuir isotherm model, whereas the NIP fit the Freundlich model. The kinetic study revealed that pseudo-second-order was the appropriate kinetic model for both DBP-IP and NIP. The imprinting factor of DBP-IP was determined by a selectivity study and showed a higher value of k_d, which proved that DBP-IP was more selective toward DBP compared to NIP.

Keywords: molecularly imprinted polymer, dibutyl phthalate, adsorption study

Abstrak

Penggunaan ftalat yang meluas menimbulkan kebimbangan mengenai kesannya terhadap kesejahteraan manusia dan haiwan. Oleh itu, kajian ini bertujuan untuk meneroka potensi pembentukan polimer molekul tercetak dengan mengkaji ciri fizikal dan keupayaan penjerapannya melalui analisis pengikatan. Kajian ini mensintesis polimer molekul tercetak-dibutil ftalat (DBP-IP)

melalui pempolimeran pemendakan menggunakan dibutil ftalat (DBP-IP), asid metakrilik, dan divinilbenzena-80 masing-masing sebagai templat, monomer berfungsi dan taut-silang. Polimer telah dicirikan menggunakan spektroskopi inframerah transformasi Fourier, pengimbasan mikroskop elektron dan analisis luas permukaan dan keliangan. Prestasi polimer tersintesis telah dinilai melalui eksperimen pengikatan semula secara kelompok. Oleh itu, kaedah spektrofotometri kinetik digunakan untuk menerangkan penentuan molekul DBP berdasarkan kesan penjerapannya ke atas polimer. Kesan pH, kepekatan, dan masa yang diambil telah disiasat untuk mendedahkan mekanisme yang mungkin melalui kajian isoterma dan kinetik penjerapan. Hasilnya menunjukkan bahawa DBP-IP mempunyai kecekapan penjerapan yang baik dalam larutan berasid dengan kepekatan yang lebih rendah. Peratusan penyingkiran maksimum untuk DBP-IP dan NIP masing-masing mencapai 90% dan 53%. Kajian mengenai penjerapan menunjukkan bahawa DBP-IP mengikuti model isoterma Langmuir, manakala NIP sesuai dengan model Freundlich. Kajian kinetik menunjukkan bahawa pseudo-order kedua adalah model kinetik yang sesuai untuk kedua-dua DBP-IP dan NIP. Faktor pencetakan DBP-IP ditentukan oleh kajian selektiviti dan menunjukkan nilai k_d yang lebih tinggi, yang membuktikan bahawa DBP-IP lebih selektif terhadap DBP berbanding NIP.

Kata kunci: polimer molekul tercetak, dibutil ftalat, kajian penjerapan

Introduction

Phthalate esters are characterized as phthalates with a high molecular weight [1]. Phthalates (PAEs) are colorless, water-insoluble synthetic organic chemicals with moderate volatility. PAEs are commonly utilized in plastics, fertilizers, insecticides, toys, cosmetics, and other industries due to their potential to improve materials' clarity, strength, plasticity, and durability [2]. Their broad application and exposure have prompted health concerns. Exposure to PAEs is connected with a variety of illnesses, although reproductive abnormalities are the most prominent [3]. Dibutyl phthalate (DBP), a form of phthalate ester (PAE), is extensively used in industry, medicine, agriculture, and animal husbandry. DBP is a pervasive environmental contaminant because it does not react chemically with the molecular bonds of the polymer matrix [4]. DBP could potentially taint and diminish the quality of produce. People are exposed to this pollutant by food, inhalation, and skin contact with agricultural products containing the substance. Hence, the potential health risk is not an insignificant concern [5]. DBP is a low molecular weight phthalate with a strong inflammatory potential relative to other phthalates and a reasonably high concentration in indoor air, making it a good option for investigation. They effectively observed strong modulatory effects of DBP on the reactions elicited by inflammatory stimuli in vitro [6].

The accumulation of DBP in vegetables may potentially have negative effects on their quality. For example, Kong and colleagues (2018), have investigated the effects of DBP on a soil-vegetable ecosystem. The results demonstrated that DBP may accumulate in plant tissues, and the accumulation effect was exacerbated by greater DBP contamination levels in soils. It was found that DBP concentration in soils, plastic film, and vegetables ranged from 0.42-1.23 mg/kg, 2.3-11.2 mg/kg, and 0.11-2.95 mg/kg, respectively. DBP accumulation lowered the quality of vegetables in a variety of ways, including a reduction in soluble protein content and an increase in nitrate level. Research has shown that DBP pollution can enhance the direct and indirect health risks of vegetables, particularly when DBP concentrations in the soil are elevated. More study is required to decrease the DBP concentration in vegetables and enhance vegetable quality, hence reducing the health risk [5].

Molecularly imprinted polymers (MIPs) are synthetic polymers possessing specific cavities designed for target molecules [7]. The production of MIPs begins with the placement of functional monomers around template molecules (which serve as an analogue of the eventual target analyte). Monomers may engage in covalent or non-covalent interactions with template sites. Around the template, they are then polymerized and cross-linked, resulting in a highly cross-linked, three-dimensional network polymer. After polymerization, the template is eliminated, leaving holes comparable in size and shape to the template molecule and prepared for precise recombination with the template [8]. Generally, MIPs are simple to produce and substantially less expensive than natural antibodies. They have exceptional mechanical qualities and a high degree of stability. In addition, molecular imprinting can be used

for a wide variety of analytes, enabling the development of sensors targeting small molecules, such as medicines, insecticides, peptides, and sugars, as well as bigger chemical compounds and bio-analytes, such as viruses, erythrocytes, and immunoglobulins [9].

Different polymerization methods can be considered to control the morphology and physicochemical stability of the resulting MIPs. In this study, precipitation polymerization was chosen for MIP preparation. The commonly used polymerization technique in the process of making a MIP is bulk polymerization due to its simplicity and lack of expertise requirement [10]. Bulk polymerization is a very convenient and easy way to produce polymers. No particular skills or sophisticated equipment are required and it has proved its interest for the development of new imprinting strategies [11]. According to He and co-workers [12], during the preparation process, only the monomers, template and cross-linkers polymerize to form polymers without any solvent or other dispersants. Polymerization needs to be initiated by a chemical initiator, light, heat, or radiation. The method is simple and avoids other solvents used in the polymerization process. However, the polymers obtained via this method are uneven and irregular. In the follow-up application, the polymers need to be further ground and sieved, which could destroy the structure of the polymers and the imprinting sites. More importantly, the imprinting sites are deeply embedded in the highly cross-linked polymers. It is disadvantageous to elution and recombination, resulting in a slow mass transfer rate, long equilibrium time and less binding.

MIPs have numerous benefits, including rapid and simple synthesis, good chemical and thermal stability, low fabrication cost, and high specificity [13]. Polymers can also be used repeatedly without losing their "memory effect" if printed on a template. MIPs are not proteins and are therefore resistant to proteolysis and bacterial destruction [14]. This study focuses on the recognition of dibutyl phthalate to prepare new materials that serve as effective sorbents with desired properties to overcome their limitations.

Materials and Methods

Materials

The chemicals used in this experiment were dibutyl phthalate (DBP), silica gel, methacrylic acid (MAA), divinylbenzene-80 (DVB-80), azobisisobutyronitrile (AIBN) and hydroquinone obtain from Sigma Aldrich supplier, whereas acetonitrile, toluene, methanol, and acetic acid were supplied by R&M Chemicals. Before use, MAA and DVB-80 were purified and AIBN was re-crystallized from methanol.

Synthesis of the polymers

The synthesis of DBP-IP was carried out by the precipitation polymerization method [15]. In general, the template, DBP (1 mmol), was dissolved in a mixture of acetonitrile and toluene (ratio 3:1) in a 250 mL Nalgene bottle. This was followed by the addition of the functional monomer, MAA (4 mmol), and the crosslinker, DVB-80 (20 mmol). Finally, the initiator, AIBN (0.4 g), was added. The solution was deoxygenated by bubbling nitrogen gas through the solution for about 5 minutes in an ice bath and it was then sealed under nitrogen. The Nalgene bottle was then placed on a roller-bed incubator. The temperature ramped from room temperature to 60 °C over a period of approximately 2 hours and then kept constant at 60 °C for 48 hours thereafter. After the polymerization was completed, the Nalgene bottle was cooled to room temperature and a bit of hydroquinone is added to the milky suspension of the polymer particles. It was then filtered then washed with acetonitrile (2 x 20 mL) and methanol (20 mL). The remaining template and unreacted monomers were removed by Soxhlet Extraction with methanol and acetic acid in a 9:1 ratio for 24 hours. The polymer was transferred to a pre-weighed vial and dried to constant mass in vacuo at 40 °C. Finally, the non-imprinted polymer (NIP) as a control sample was prepared using the same method but in the absence of the template.

Characterization of the polymers

The polymers were characterized by attenuated total reflection-Fourier transform infrared spectroscopy (ATR-FTIR). The spectra were recorded from 500 cm^{-1} to 4000 cm^{-1}. Scanning Electron Microscopy (SEM) was then used to examine the surface morphology of the

polymers. Each polymer was affixed to the stubs and gold-coated for protection against the electron beam. Next, the determination of the specific surface area, pore volume and pore diameter were performed by porosity analyzer using Bruner-Emmett-Teller (BET) and Barrett-Joyner-Halenda (BJH) technique.

Adsorption isotherm studies

The adsorption studies were conducted by batch rebinding experiment, which was performed in an aqueous medium. First, 2 mg of DBP-IP was prepared and mixed with a different concentration of DBP solution (1, 3, 5, 7, 9 ppm) while maintaining other parameters at optimal conditions. After the adsorption process, the DBP solution was analyzed using a UV-Vis spectrometer to determine the remaining DBP molecule by observing its final concentration. Then, the percentage removal and adsorption capacity of DBP-IP towards DBP was calculated using equations (1) and (2), respectively [16]:

$$\% \text{ removal } = \frac{C_i - C_f}{C_i} \times 100 \quad (1)$$

$$Q_e = \frac{(C_i - C_f)V}{W} \quad (2)$$

In the equations above, C_i and C_f are initial and final concentrations (mg/L) of DBP solutions, respectively, Q_e (mg/g) is the quantity of total adsorption of DBP molecules, V (L) is the volume of the solution and W (g) is the weight of polymers. The relation between the equilibrium concentration and absorbate analyte was then described by an adsorption isotherm study. The equilibrium data were fitted into Langmuir and Freundlich isotherm models. The Langmuir and Freundlich equations can be written as in equations (3) and (4), respectively [17]:

$$\frac{C_e}{Q_e} = \frac{1}{Q_o} C_e + \frac{1}{Q_o K_L} \quad (3)$$

$$\text{In } Q_e = \text{ In } K_F + \frac{1}{n} \text{ In } C_e \quad (4)$$

where C_e is the equilibrium concentration of the adsorbents (mg/L), Q_e is the equilibrium adsorption capacity (mg/L), Q_o is the maximum adsorption capacity of the adsorbents (mg/g), K_L is the Langmuir isotherm constant, K_F is the Freundlich constant and n is the value of the heterogeneity parameter. Linearized forms of the isotherm models were plotted and the related coefficient (R^2) was compared. The favorability of the Langmuir isotherm was expressed by a dimension constant called the separation factor (RL), as shown in equation (5);

$$RL = \frac{1}{1+K_L(C_e)} \quad (5)$$

where RL values indicate the adsorption to be unfavourable when RL > 1, linear when RL = 1, favourable when 0 < RL > 1, and irreversible when RL = 0 [16].

Adsorption kinetic studies

The kinetic consideration was further investigated through the Pseudo-first-order and Pseudo-second-order equation models to fit the experimental data and investigated the reaction rate of DBP adsorption towards DBP-IP and NIP. The experiments were conducted using 1 ppm of DBP solution mixed with 2 mg of DBP-IP. The kinetics of DBP uptake by DBP-IP were analyzed using a UV-Vis spectrometer. The time was set at 0 to 180 min. The Pseudo-first-order can be calculated using the following equation (6):

$$\text{In}(Q_e - Q_t) = \text{In } Q_e - k_1 t \quad (6)$$

Meanwhile, the Pseudo-second-order can be defined according to the following equation (7):

$$\frac{t}{Q_t} = \frac{k_2}{k_2 Qe^2} + \frac{t}{Q_e} \quad (7)$$

where Q_t and Q_e (mg/g) represent adsorption capacities at time and equilibrium, respectively, while k_1 and k_2 represent rate constants at equilibrium [16]. Furthermore, the favorability of kinetic models was calculated by standard deviation formula, Δq (%) and relative error, RE (%) as in the following equations (8) and (9):

$$\Delta q(\%) = \sqrt{\frac{[(Q_{e,exp} - Q_{e,cal})/Q_{e,exp}]^2}{N-1}} \times 100 \quad (8)$$

$$RE(\%) = \frac{|Q_{e,cal} - Q_{e,cal}|}{Q_{e,exp}} \times 100 \quad (9)$$

where N is the amount of data points fitted to the plot, $Q_{e,exp}$ and $Q_{e,cal}$ (mg/g) are the experimental and calculated adsorption capacities, respectively. A lower Δq (%) gives the desired fitness of the polymer to the kinetic model [19].

Effect of pH

1 ppm of DBP solution was prepared, and the pH was adjusted in the range of 4, 5, 7, 8 and 10 by adding diluted HCl and NaOH. The experiment was carried out by mixing each solution with 2 mg of DBP-IP. The optimum pH for optimum adsorption was determined.

Effect of selectivity

In the selectivity study, the molecular structural analogue of Dibutyl phthalate (DBP) which is Dioctyl phthalate (DOP), was tested for the binding performance with DBP-IP. It was chosen as the competitive compound to verify the specificity of DBP-IP for DBP. Firstly, 1 ppm of analyte concentration was prepared separately and mixed with 2 mg of DBP-IP. Then, the solution was analyzed using UV-Vis spectrometer. The distribution coefficient (k_d) was calculated based on the equation (10):

$$k_d = \frac{(C_i - C_f)}{C_f}\left(\frac{V}{W}\right) \quad (10)$$

where k_d is the concentration ratio between two solutions, C_i and C_f are initial and final concentrations of each compound, respectively. V (L) is the volume of the solution and W (g) is the weight of polymers. The adsorption capacity of the polymer increases as the value of k_d increases. Selectivity coefficient (k), which indicates the selectivity of DBP over the competitive compounds was calculated based on the equation (11) below:

$$k = \frac{k_d(DBP)}{k_d(DOP)} \quad (11)$$

Relative selectivity coefficient (k') was determined by comparing the ratio of DBP-IP and NIP as equation (12) below:

$$k' = \frac{k(DBP - IP)}{k(NIP)} \quad (12)$$

Results and Discussion

Synthesis of the polymers

The experimental result showed that functional monomers, MAA strongly interacted with the template, DBP. The stability of the complexes formed by the template and functional monomer is crucial in determining the recognition properties of molecularly imprinted polymers (MIPs) [20]. Furthermore, the successful synthesis of both DBP-IP and NIP yielded white, opaque polymer monoliths, which were subsequently subjected to comprehensive characterization and binding investigations (Figure 1).

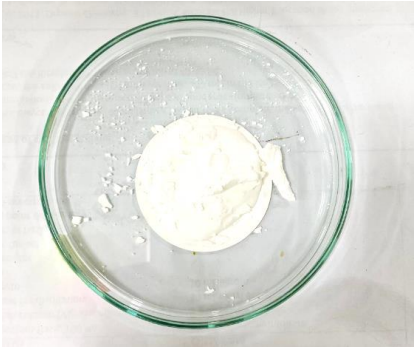

Figure 1. The synthesized of DBP-IP

FTIR characterization

The functional groups within the obtained polymer particles were identified through FTIR spectroscopy analysis of DBP-IP and NIP. A comparison of the IR spectra of DBP-IP before and after template removal, and NIP, revealed slight variations attributed to the presence of DBP as a template within the polymer matrix. Figure 2 shows the FTIR spectra of DBP, DBP-IP before and after template removal and the NIP. From the DBP spectrum in Figure 2(a), a peak of 1723.49 cm^{-1} was observed, indicating a peak for C=O stretching from the anhydride group, which represents a DBP molecule. At Figure 2(b), the intensity of the C=O absorption peak increased from 1725cm^{-1} to 1802 cm^{-1}. This is due to the strong interaction between the C=O group of the DBP and the O-H group of the MAA. While, no such spectra were observed in Figure 2(c), which shows the successful disappearance of the template molecule. The strong broad peak at Figure 2(b), (c), and (d) shows almost the same intensity at 3725.45–3745 cm^{-1}, which is attributed to the vibrating mode of O-H stretch from MAA. Besides that, peaks that appeared at 1445–1449 cm^{-1} and 2913–2920 cm^{-1} indicated the presence of the C=C (aromatic) bond and the C-H (alkane) bond, respectively. Moreover, the IR peaks obtained at 989–987 cm^{-1} show the C=C stretching vibrations because of DVB-80. Due to the high cross-linking agent in DVB-80, all polymers show similar vibration peaks with almost the same IR spectrum.

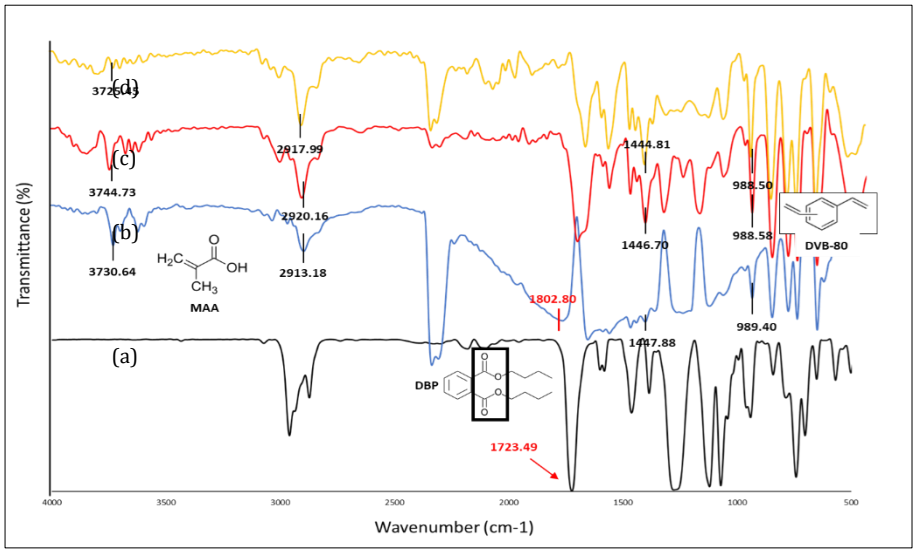

Figure 2. FTIR spectrum (a) DBP; (b) DBP-IP before; (c) DBP-IP after template removal; (d) NIP

SEM characterization

During precipitation polymerization, a dispersion of monomers, templates, and cross-linkers is achieved in a solvent of significant volume. The resulting polymer exhibits insolubility in the solvent, leading to precipitation and the formation of well-defined, spherical molecularly imprinted polymers (MIPs) [21]. Figure 3 displays scanning electron microscopy (SEM) images of non-imprinted polymer (NIP) and dibutyl phthalate-imprinted polymer (DBP-IP). The prepared polymers exhibit desirable size uniformity and distinct differences in their morphologies. Specifically, the micrographs reveal that DBP-IP, exhibiting the imprinting effect, possesses a relatively rough microstructure characterized by distinct pores embedded within the polymer matrices. In contrast, NIP samples display smoother and cleaner surfaces. The smooth surface of NIP is attributed to the creation of non-specific binding sites for the analyte, whereas the rough surface of DBP-IPs arises from the cavities formed during template removal.

Analysis of Table 1 indicates that the average particle size of DBP-IP is approximately 2.78 µm, whereas the

average particle size of spherical NIP measures 3.22 µm, thus demonstrating the influence of the template on particle size. Increased interaction between the template and monomer leads to the formation of polymer nuclei, resulting in the synthesis of polymer beads with reduced diameters [22]. Micrographs depict polymer particles exhibiting diverse sizes and shapes, with a predominance of spherical polymer particles produced using acetonitrile as a solvent [23]. The presence of DVB-80 as a cross-linker within the polymer matrix also contributes to these observations. Notably, the cross-linker imparts mechanical strength to the polymer and enhances the stability of recognition sites within the polymer matrix [24]. Consequently, the uniformity among the particles can be attributed to the combined influence of DVB-80 and the acetonitrile-toluene mixture.

Table 1. Average diameter size for spherical polymer beads

Average diameter size (µm)	NIP	DBP-IP
	3.22	2.78

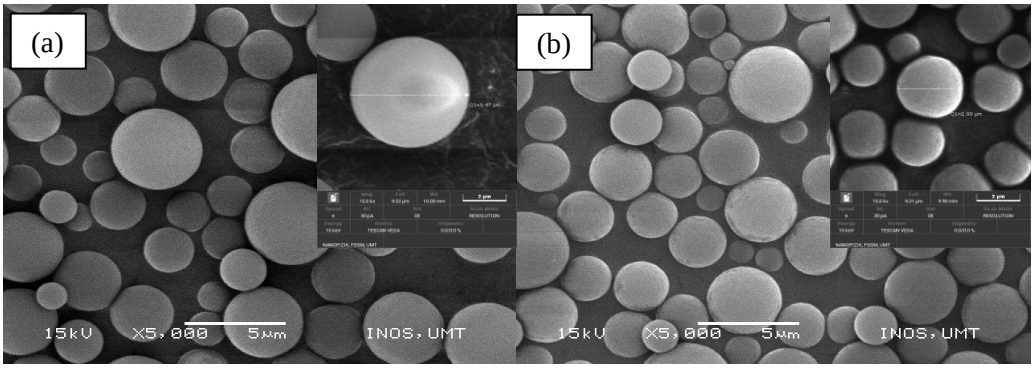

Figure 3. Polymers morphology of (a) NIP and (b) DBP-IP at magnification 5000X and 15,000X

BET surface area analysis and porosity

According to the data presented in Table 2, it is evident that DBP-IP exhibits a greater surface area in comparison to NIP, indicating its superior porosity. Porous materials are commonly classified based on the size of their pores, which fall into three categories: micropores (2 nm), mesopores (2-50 nm), and macropores (> 50 nm). From the pore diameter values listed in Table 2, it is evident that both NIP and DBP-IP belong to the mesopore category. Furthermore, DBP-IP has a larger surface area and is slightly larger in total pore volume than the NIP. The increased pore diameter of the imprinted polymer signifies a stronger imprinting effect of the templates. This also provides information about the presence of a template during the MIP synthesis, which leads to the creation of imprinted cavities.

Table 2. BET surface area, pore volume and pore diameter

P Polymers	Surface Area (m^2/g)	Pore Volume (cm^3/g)	Pore Diameter (nm)
NIP	508.89	0.2954	2.2154
DBP-IP	532.76	0.3091	2.2183

Adsorption isotherm study

In this adsorption study, the experiment was carried out at different concentrations of DBP (1, 3, 5, 7, and 9 ppm). Figure 4 shows that the maximum percentage removal achievable by DBP-IP and NIP were 90% and 53%, respectively. It is also obvious that the adsorption capacity of DBP onto the DBP-IP was significantly higher than that onto the NIP, due to the fact that the

DBP-IP had specific binding sites whereas NIP possessed non-specific binding sites for adsorption of DBP. As a result, the percentage removal of NIP is lower than DBP-IP. The binding capacity of DBP-imprinted polymer (DBP-IP) exhibited a notable decrease as the concentration of DBP increased, eventually reaching equilibrium upon reaching an initial concentration of 3 ppm. This decline can be attributed to the existence of an optimal number of binding sites within DBP-IP. Further increases in the template concentration may have led to overcrowding around DBP-IP, thus limiting the availability of binding sites. This phenomenon explains why molecularly imprinted polymers (MIPs) demonstrate reduced affinity and selectivity at high template concentrations [25]. Consequently, an increase in the initial concentration does not result in an increase in the binding capacity of DBP-IP.

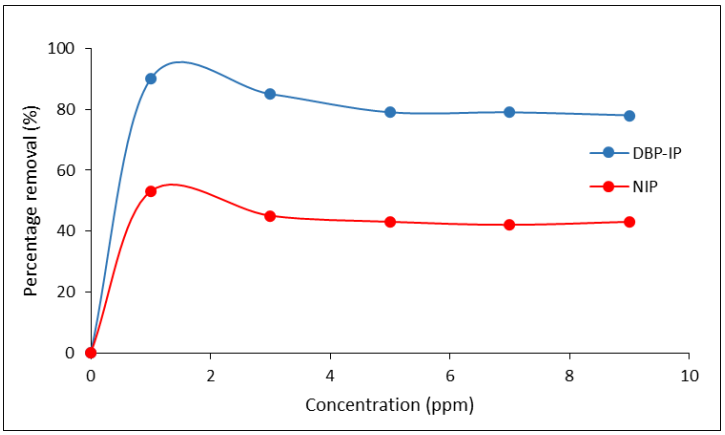

Figure 4. Effect of initial concentration on adsorption DBP by DBP-IP and NIP

Equilibrium data, referred to as an adsorption isotherm, serves as a fundamental requirement for the design of adsorption systems [26]. To validate the Langmuir isotherm, the plot of Ce/Qe (mg/g) versus Ce (mg/L) was employed. From the Langmuir expression, the Langmuir constants Qo and KL were determined and are provided in Table 3. Figure 5 illustrates that the correlation coefficient value for DBP-imprinted polymer (DBP-IP) (R^2=0.9935) is higher than that for non-imprinted polymer (NIP) (R^2=0.0563), indicating a strong linear relationship for DBP-IP. The key characteristics of the Langmuir isotherm can be expressed through the dimensionless constant separation factor RL, which was calculated. The RL values for DBP adsorption onto DBP-IP and NIP were 0.084 and 1.528, respectively, signifying the favorable nature of DBP adsorption onto DBP-IP. The equilibrium data were further analyzed using the linearized form of the Freundlich isotherm by plotting log Qe versus log Ce. The calculated Freundlich isotherm constants for DBP-IP and NIP are presented in Table 3. As depicted in Figure 6, the correlation coefficient values for DBP-IP (R^2=0.0918) and NIP (R^2=0.9963) are displayed, indicating high correlation coefficients for NIP and adherence of the adsorption process to the Freundlich model. However, according to the results in Table 3, the values of n for DBP-IP are greater than those for NIP, suggesting favorable adsorption of DBP on DBP-IP. This finding is in good agreement with the RL value. The magnitude of the Freundlich constant indicates the ease of DBP uptake from the aqueous solution [26].

Based on the analysis of Figure 5, Figure 6, and Table 3, it can be deduced that the Langmuir isotherm model exhibited greater suitability in describing the adsorption behavior of DBP-IP, while the Freundlich isotherm model demonstrated enhanced suitability for characterizing the adsorption of NIP. This inference is supported by the observation of high correlation coefficients associated with these models.

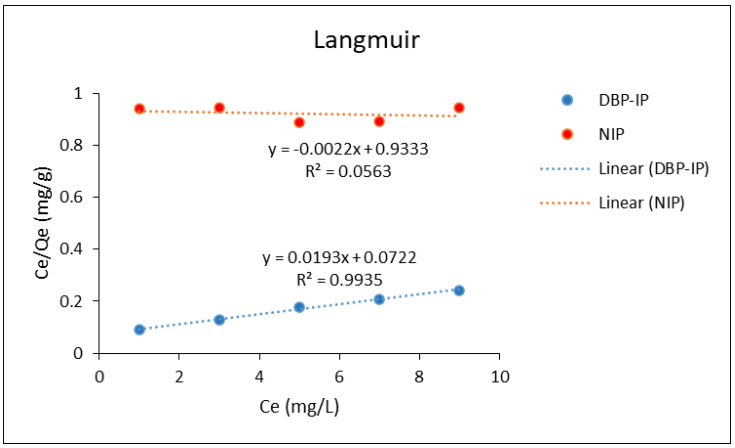

Figure 5. Adsorption isotherm of DBP-IP and NIP using Langmuir model

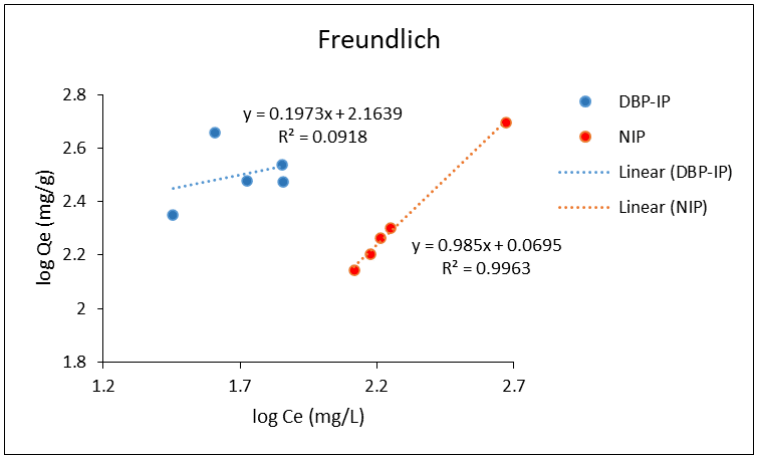

Figure 6. Adsorption isotherm of DBP-IP and NIP using Freundlich model

Table 3. Langmuir and Freundlich isotherms constant for DBP-IP and NIP

Polymers	Isotherm Model	RL	Q_o (mg/g)	K_L (L/mg)	n	K_F (mg/g)
MIP	Langmuir	0.085	51.918	0.266	-	-
	Freundlich	-	-	-	5.069	1.575
NIP	Langmuir	1.536	-461.741	$-2.320 \times 10^{-}$	-	-
	Freundlich	-	-	-	1.0152	1.174

Adsorption kinetic study

The impact of contact time on the adsorption of dibutyl phthalate (DBP) by DBP-IP and NIP was investigated by combining 2 mg of polymer with a 1 ppm DBP solution for a duration ranging from 0 to 180 minutes. Analysis of Figure 7 reveals that the adsorption rate exhibited a rapid initial stage within the first 80 minutes, followed by a gradual decline until reaching equilibrium. This behavior can be attributed to the initial occupation of the abundant imprinted sites and cavities on the polymer surface, after which DBP molecules needed to diffuse from the external to the internal sites, leading to a longer contact time requirement [27]. The adsorption equilibrium was ultimately attained at approximately 160 minutes for DBP-IP and 170 minutes for NIP. Further extension of the contact time did not result in any substantial changes in adsorption efficiency, which remained relatively constant. Notably, the efficiency of NIP was found to be the lowest, likely due to the absence of complementary binding sites [25].

The determination of kinetic constants for the adsorption of dibutyl phthalate (DBP) by DBP-IP and NIP can be obtained from the linear plots of log ($Q_e - Q_t$) versus t for the pseudo-first-order model and t/Q_t versus t for the pseudo-second-order model. The correlation coefficients for the pseudo-first-order model are depicted in Figure 8, with values of $R^2 = 0.9147$ and $R^2 = 0.9325$ for DBP-IP and NIP, respectively. Conversely, in Figure 9, the correlation coefficients for the pseudo-second-order model were found to be higher, with R^2 values of 0.9983 for DBP and 0.9612 for NIP. Thus, the pseudo-second-order model exhibited greater relevance. Both DBP-IP and NIP followed pseudo-second-order kinetics in their adsorption process, suggesting that the adsorption was primarily driven by a chemical process, which likely acted as the rate-limiting step [28]. Analysis of Table 4 confirms that the adsorption of DBP-IP and NIP adhered to pseudo-second-order kinetics, as evidenced by the favorable agreement between the experimental ($Q_{e,\ exp}$) and calculated ($Q_{e,\ cal}$) values. Moreover, to validate the proposed model, Δ_q and RE values were assessed at lower percentage values, ultimately confirming the best fitness of the pseudo-second-order model for the kinetic adsorption of DBP onto DBP-IP.

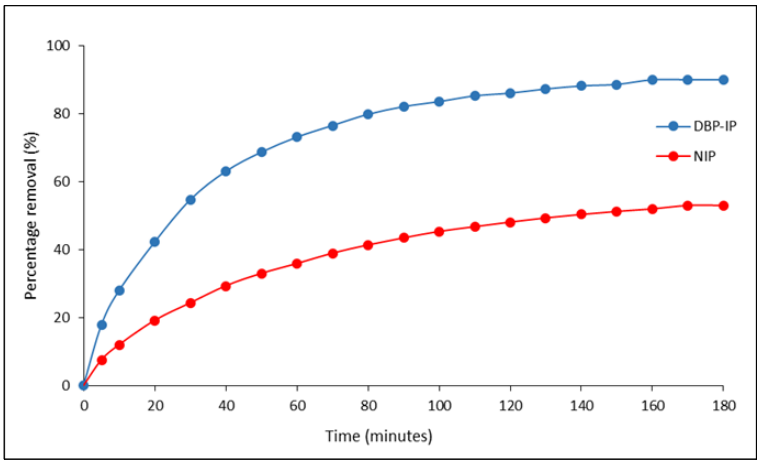

Figure 7. Effect of contact time on adsorption DBP by DBP-IP and NIP

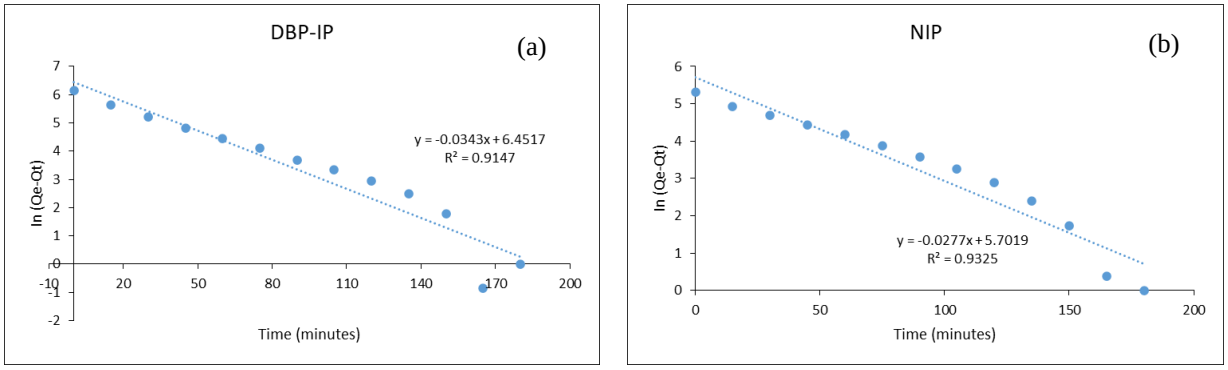

Figure 8. Pseudo-first-order plots for adsorption of DBP by (a) DBP-IP and (b) NIP

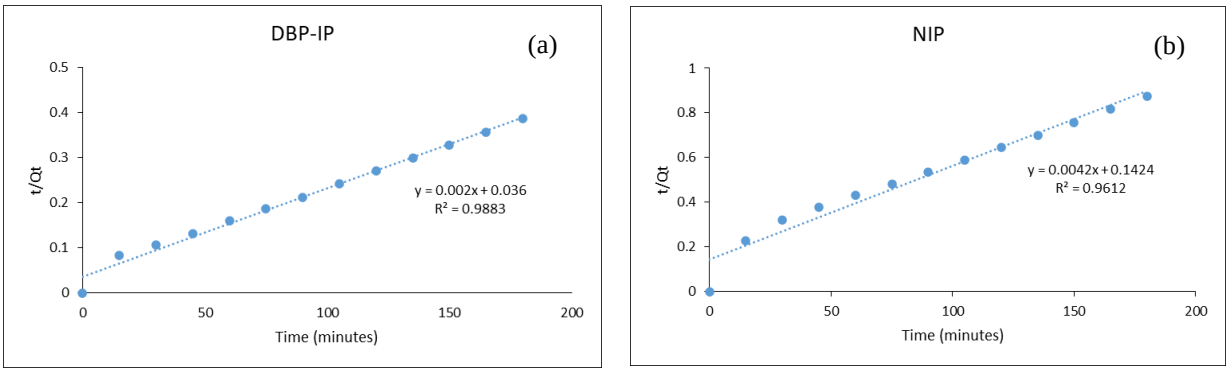

Figure 9 Pseudo-second-order plots for adsorption of DBP by (a) DBP-IP and (b) NIP

Table 4. Kinetic constant for adsorption of DBP by DBP-IP and NIP

Polymers	**Model**	**$Q_{e,\ exp}$ (mg/g)**	**$Q_{e,\ cal}$ (mg/g)**	**Δ_q (%)**	**RE (%)**	**k**
DBP-IP	Pseudo-first-order	462.469	633.779	10.69	37.04	0.034
	Pseudo-second-order		500.000	2.34	8.11	$1.1X10^{-4}$
NIP	Pseudo-first-order	203.700	299.439	13.58	47.00	0.028
	Pseudo-second-order		238.095	4.87	16.88	$1.2X10^{-4}$

Effect of pH

The pH of the solution plays a crucial role in influencing the ionization of the adsorbate and altering the surface charge of the molecularly imprinted polymer (MIP). Consequently, the impact of pH should be assessed on a case-by-case basis, as it is specific to the particular MIP employed and requires independent evaluation [27]. In order to investigate the effect of pH on the binding capacity of the polymer, experiments were conducted at different pH levels by varying the pH of the template solution from acidic to basic conditions. 1 ppm of DBP solution was prepared, and the pH was adjusted in the range of 4, 5, 7, 8 and 10 by adding diluted HCl and NaOH. The experiment was carried out by mixing each solution with 2 mg of DBP-IP. The optimum pH for optimum adsorption was determined. As depicted in Figure 10, the highest percentage removal (90%) was achieved under acidic pH conditions, while the removal efficiency decreased (30%) as the pH increased, indicating a shift towards basic conditions. This behavior could potentially be attributed to the hydrogen bonding interaction between the carboxylic group on the surface of the methacrylic acid (MAA) and the functional group of dibutyl phthalate (DBP).

Furthermore, it was observed that an increase in solution pH led to a decrease in removal efficiency. This can be attributed to the pH-dependent hydrolysis of DBP, wherein DBP undergoes hydrolysis to form phthalic acid and protonated phthalic acid in acidic solutions. The concentration of hydrolysis products increases with increasing acidity, resulting in an increase in positive charges [30]. The carbonyl group of the phthalate moiety exhibits nucleophilic properties and readily forms a bond with H^+ ions, acquiring a positive charge. Consequently, electrostatic repulsion occurs, leading to a decrease in the rate of removal [31]. Thus, based on these observations, a pH of 4 was determined as the optimal pH for the study.

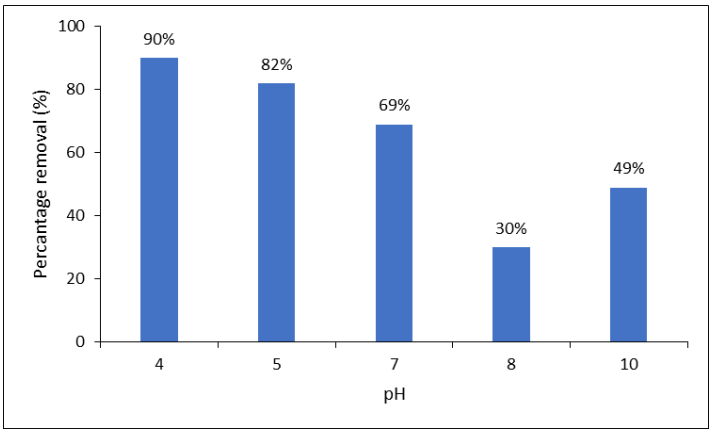

Figure 10. Effect of pH on adsorption of DBP by DBP-IP

Effect of selectivity

The adsorption selectivity of the DBP-imprinted polymer (DBP-IP) towards dibutyl phthalate (DBP) and its structural analog, dioctyl phthalate (DOP), as a competitive substrate was investigated to evaluate the complementary interaction between the polymer and template. The adsorption experiments for each adsorbate were conducted under identical conditions, with all adsorbates maintained at a concentration of 1 ppm. As depicted in Figure 11, DBP-IP exhibited a significantly higher removal rate for DBP compared to DOP, indicating its pronounced sorption selectivity towards DBP. A comparison of the removal rates between DBP-IP and non-imprinted polymer (NIP) adsorbents for each adsorbate revealed that DBP-IP displayed specificity towards DBP while exhibiting a lack of specificity towards other adsorbates. Conversely, the NIP adsorbents displayed similar removal rates for all adsorbates, albeit with an 11% lower removal rate compared to DBP-IP for DBP adsorbates. This observation can be attributed to the non-specific nature of the imprinting sites within the polymer network [32].

Analysis of Table 5 indicates that DBP exhibited higher k_d values in DBP-IP compared to DOP, signifying a higher specificity for DBP. In contrast, NIP displayed higher k_d values for DOP compared to DBP, suggesting the presence of non-specific cavities within NIP. Additionally, the k values indicate the selective behavior of the polymer towards the template in the presence of other molecules. Larger k values indicate higher selectivity of the polymer towards the template relative to other molecules. In the case of DBP-IP, the k values were higher compared to NIP, indicating the selective behavior of DBP-IP towards DBP.

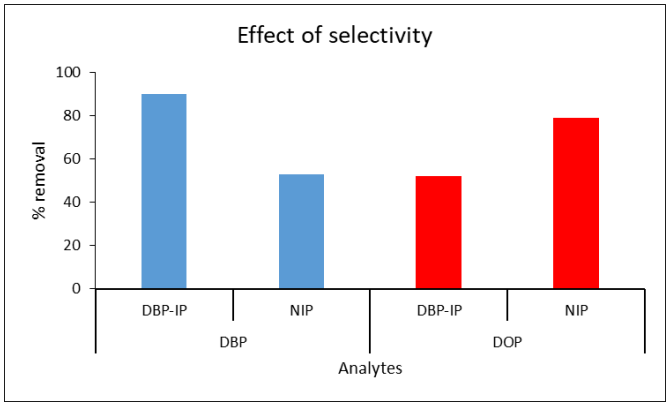

Figure 11. Effect of selectivity of DBP-IP and NIP toward the DBP and DOP

Table 5. Selectivity constants for DBP-IP and NIP toward the DBP and DOP

Analytes	DBP-IP		NIP		
	k_d	k	k_d	k	k'
DBP	13.826	-	1.719	-	-
DOP	1.614	8.565826	5.565	0.3089	27.72819

Conclusion

In this study, DBP-imprinted polymer (DBP-IP) and non-imprinted polymer (NIP) were successfully synthesized via precipitation polymerization and employed as adsorbents for dibutyl phthalate (DBP) detection. The physical and chemical characteristics of the synthesized polymers were analyzed using FTIR, SEM, and BET techniques. Remarkably, DBP-IP exhibited superior performance in adsorbing DBP, achieving a remarkable removal efficiency of up to 90%, surpassing the effectiveness of NIP. The adsorption behavior of DBP-IP conformed well to the Langmuir adsorption model, while NIP followed the Freundlich adsorption model. Furthermore, the adsorption kinetics of both DBP-IP and NIP followed a pseudo-second-order process. Equilibrium adsorption was attained at 160 minutes for DBP-IP and 170 minutes for NIP. Notably, a selectivity study revealed that the value of k_d (distribution coefficient) for DBP-IP in DBP solution was higher compared to that in dioctyl phthalate (DOP) solution, indicating the excellent selectivity of DBP-IP towards DBP and successful imprinting of the target molecule.

Acknowledgments

We would like to thank the Universiti Malaysia Terengganu especially the Faculty of Science and Marine Environment for providing the facilities for undertakings works.

References

1. Donia, R., Abdel-Ghaffar, A.-R., Sultan, E., Hassanin, E., and Borai, I. (2021). Evaluation of sex hormones in male and female egyptian population naturally exposed to dibutyl phthalate: a cross-sectional study. *Egyptian Journal of Pure and Applied Science*, 59(1): 1-8.
2. Zhang, Y., Jiao, Y., Li, Z., Tao, Y., and Yang, Y. (2021). Hazards of phthalates (PAEs) exposure: A review of aquatic animal toxicology studies. *Science of the Total Environment*, 771: 145-418.
3. Hlisníková, H., Petrovičová, I., Kolena, B., Šidlovská, M., and Sirotkin, A. (2020). Effects and mechanisms of phthalates' action on reproductive processes and reproductive health: A literature review. *International Journal of Environmental Research and Public Health*, 17(18): 6811.
4. Meng, H., Yao, N., Zeng, K., Zhu, N., Wang, Y., Zhao, B., and Zhang, Z. (2022). A novel enzyme-free ratiometric fluorescence immunoassay based on silver nanoparticles for the detection of dibutyl phthalate from environmental waters. *Biosensors*, 12(2): 125.
5. Kong, X., Jin, D., Jin, S., Wang, Z., Yin, H., Xu, M., and Deng, Y. (2018). Responses of bacterial community to dibutyl phthalate pollution in a soil-vegetable ecosystem. *Journal of Hazardous Materials*, 353: 142-150.
6. Maestre-Batlle, D., Pena, O. M., Huff, R. D., Randhawa, A., Carlsten, C., and Bølling, A. K. (2018). Dibutyl phthalate modulates phenotype of granulocytes in human blood in response to inflammatory stimuli. *Toxicology Letters*, 296: 23-30.
7. Huang, D.-L., Wang, R.-Z., Liu, Y.-G., Zeng, G.-M., Lai, C., Xu, P., Lu, B.-A., Xu, J.-J., Wang, C., and Huang, C. (2014). Application of molecularly imprinted polymers in wastewater treatment: a review. *Environmental Science and Pollution Research*, 22(2): 963-977.
8. Sarafraz-Yazdi, A., and Razavi, N. (2015). Application of molecularly-imprinted polymers in solid-phase microextraction techniques. *TrAC Trends in Analytical Chemistry*, 73: 81-90.
9. Wackerlig, J., and Lieberzeit, P. A. (2015). Molecularly imprinted polymer nanoparticles in chemical sensing – Synthesis, characterisation and

application. *Sensors and Actuators B: Chemical*, 207: 144-157.

10. Hasanah, A. N., Soni, D., Pratiwi, R., Rahayu, D., Megantara, S., and Mutakin. (2020). Synthesis of diazepam-imprinted polymers with two functional monomers in chloroform using a bulk polymerization method. *Journal of Chemistry*, 2020: 1-8.
11. Branger, C., Meouche, W., and Margaillan, A. (2013). Recent advances on ion-imprinted polymers. *Reactive and Functional Polymers*, 73(6): 859-875.
12. He, S., Zhang, L., Bai, S., Yang, H., Cui, Z., Zhang, X., and Li, Y. (2021). Advances of molecularly imprinted polymers (MIP) and the application in drug delivery. *European Polymer Journal*, 143 : 110-179.
13. Majdinasab, M., Daneshi, M., and Louis Marty, J. (2021). Recent developments in non-enzymatic (bio)sensors for detection of pesticide residues: Focusing on antibody, aptamer and molecularly imprinted polymer. *Talanta*, 232: 122-397.
14. Canfarotta, F., Cecchini, A., and Piletsky, S. (2018). Nano-sized molecularly imprinted polymers as artificial antibodies. *Polymer Chemistry Series*, 1-27.
15. Mohajeri, S. A., Karimi, G., Aghamohammadian, J., and Khansari, M. R. (2011). Clozapine recognition via molecularly imprinted polymers; bulk polymerization versus precipitation method. *Journal of Applied Polymer Science*, 121(6): 3590-3595.
16. Yusof, N. F., Mehamod, F. S., and Mohd Suah, F. B. (2019). Fabrication and binding characterization of ion imprinted polymers for highly selective Co^{2+} ions in an aqueous medium. *Journal of Environmental Chemical Engineering*, *7*(2): 103007.
17. Ayawei, N., Ebelegi, A. N., and Wankasi, D. (2017). Modelling and interpretation of adsorption isotherms. *Journal of Chemistry*, 2017: 1-11.
18. Abdullah, Alveroglu, E., Balouch, A., Khan, S., Mahar, A. M., Jagirani, M. S., and Pato, A. H. (2021). Evaluation of the performance of a selective magnetite molecularly imprinted polymer for extraction of quercetin from onion samples. *Microchemical Journal*, 162: 105849.
19. Habibah, N., Jusoh, S., Faizatul, S., Mehamod, Yusof, N., Mutalib, A., Jani, M., Bukhari, F., Suah, M., Ariffin, M., and Zulkefli, N. (2022). Preparation and adsorption studies of molecularly imprinted polymer for selective recognition of tryptophan. *Malaysian Journal of Analytical Sciences*, 26: 215-228.
20. Fan, D., Jia, L., Xiang, H., Peng, M., Li, H., and Shi, S. (2017). Synthesis and characterization of hollow porous molecular imprinted polymers for the selective extraction and determination of caffeic acid in fruit samples. *Food Chemistry*, 224: 32-36.
21. Lu, H., Tian, H., Wang, C., and Xu, S. (2020). Designing and controlling the morphology of spherical molecularly imprinted polymers. *Materials Advances*, 1(7): 2182-2201.
22. Yoshimatsu, K., Reimhult, K., Krozer, A., Mosbach, K., Sode, K., and Ye, L. (2007). Uniform molecularly imprinted microspheres and nanoparticles prepared by precipitation polymerization: The control of particle size suitable for different analytical applications. *Analytica Chimica Acta*, 584(1): 112-121.
23. Esfandyari-Manesh, M., Javanbakht, M., Atyabi, F., Badiei, A., and Dinarvand, R. (2011). Effect of porogenic solvent on the morphology, recognition and release properties of carbamazepine-molecularly imprinted polymer nanospheres. *Journal of Applied Polymer Science*, 121(2): 1118-1126.
24. Alexander, C., Andersson, H. S., Andersson, L. I., Ansell, R. J., Kirsch, N., Nicholls, I. A., O'Mahony, J., and Whitcombe, M. J. (2006). Molecular imprinting science and technology: a survey of the literature for the years up to and including 2003. *Journal of Molecular Recognition*, 19(2): 106-180.
25. Bakhtiar, S., Bhawani, S. A., and Shafqat, S. R. (2019). Synthesis and characterization of molecular imprinting polymer for the removal of 2-phenylphenol from spiked blood serum and river water. *Chemical and Biological Technologies in Agriculture*, 6(1): 10-15.

26. Singh, D. K., and Mishra, S. (2010). Synthesis and characterization of Hg(II)-ion-imprinted polymer: Kinetic and isotherm studies. *Desalination*, 257(1-3): 177-183.
27. Wahab, M. A., Jellali, S., & Jedidi, N. (2010). Ammonium biosorption onto sawdust: FTIR analysis, kinetics and adsorption isotherms modelling. *Bioresource Technology*, 101(14): 5070-5075.
28. Wang, H., Yuan, L., Zhu, H., Jin, R., and Xing, J. (2018). Comparative study of capsaicin molecularly imprinted polymers prepared by different polymerization methods. *Journal of Polymer Science Part A: Polymer Chemistry*, 57(2): 157-164.
29. Luo, X., Zhan, Y., Huang, Y., Yang, L., Tu, X., & Luo, S. (2011). Removal of water-soluble acid dyes from water environment using a novel magnetic molecularly imprinted polymer. *Journal of Hazardous Materials*, 187(1-3): 274-282.
30. Gao, M., Gong, X., Lv, M., Song, W., Ma, X., Qi, Y., and Wang, L. (2016). Effect of temperature and pH on the sorption of dibutyl phthalate on humic acid. *Water, Air, & Soil Pollution*, 227(2): 55.
31. Tsang, P. keung, Fang, Z., Liu, H., and Chen, X. (2008). Kinetics of adsorption of di-n-butyl phthalate (DBP) by four different granule-activated carbons. *Frontiers of Chemistry in China*, 3(3): 288-293.
32. Yu, Q., Deng, S., and Yu, G. (2008). Selective removal of perfluoro octane sulfonate from aqueous solution using chitosan-based molecularly imprinted polymer adsorbents. *Water Research*, 42(12): 3089-3097.